*INT. J. BIOL. BIOTECH.*, 15 (3): 483-491, 2018.

# ANTIOXIDANT ACTIVITY OF AZO GLYCOL DERIVATIVE AND THEIR CU COORDINATES

**Hamdullah Khadim Sheikh[1]*, Merrick Pierson-Smela[2], Tanzila Arshad[1], Mehdi Hassan Kazmi[1], Sadia Farheen[3] and Mehreen Lateef [4]**

[1]*Department of Applied Chemistry, University of Karachi, Karachi-75270,*
[2] *Department of Chemistry, University of Minnesota.*
[3] *Pakistan Council of Scientific & Industrial Research (*PCSIR*) Laboratories Complex, Karachi.*
[4] *Bahria University Medical & Dental College, Karachi.*
Corresponding: hamdullah.khadim.sheikh@gmail.com

## ABSTRACT

Three novel metal derivatives of azo glycol derivatives **(11-13)** have been synthesized through metal coordination of diol moiety of azo glycol molecules with Cu. The glycol molecules were found to be highly active for 2, 2-diphenyl-1-picrylhydrazyl (DPPH) radical scavenging. Metal coordinates **(11-13)** showed less antioxidant activity than ligands themselves. Electronic spectral transitions are designated by time dependent density functional theory (TD-DFT) calculations. Molecular dipole moment was also calculated.

**Key-words**: Glycerol, Metal coordination, radical scavenging, TD-DFT, Azo, Dipole moment.

## INTRODUCTION

We previously reported the synthesis of 1, 2-diol azo dyes (Sheikh and Kazmi, 2017). The molecules were designed to be compact and planar chromophores bonded with glycerol, capable of forming strong H-bonds. In this research work, the diol sites of the same series of molecules are metal coordinated. Glycol molecules themselves **(8-10)** showed high antioxidant activity, which got slightly decreased by metal coordination at glycol lewis basic sites. Metal corrdinated molecular structures are shown in (Fig **1**).

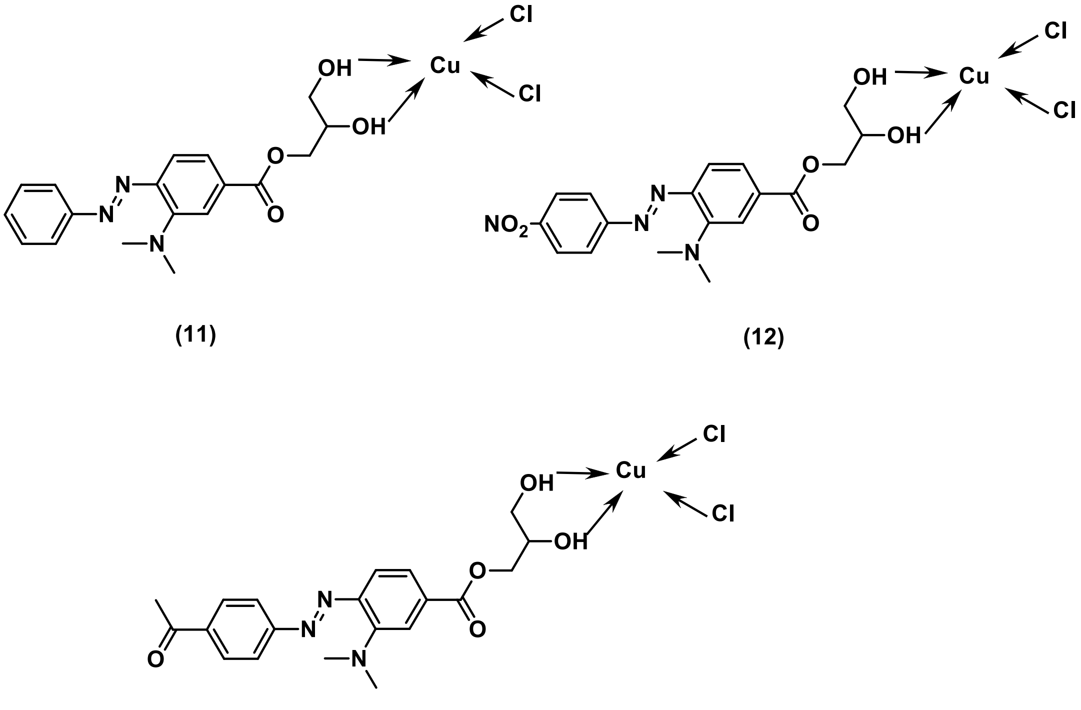

(11)

(12)

(13)

Fig 1. Molecular Structures of (11-13).

Reactive oxygen species (ROS) are generated in the body due to insufficient reduction of excess oxygen. The most common ROS are superoxide anion radical, perhydroxyl radical, hydrogen peroxide and hydroxyl radical (HO) (Bagchi and Puri, 1998) ROS can profoundly damage the cells which lead to different oxidative stress related diseases such as Alzheimer (Christen, 2000) Parkinson, cataracts, and DNA damage leadng to carcinogenesis, inflammatory diseases, atherosclerosis (Rice-Evans and Diplock, 1991) and multiple sclerosis (Armstrong *et al*., 1985). Antioxidant molecules inhibit the oxidative stress which is normal but destructive physiological process. Examples include variety of natural antioxidants e.g. vitamins C and E, flavonoids and alkaloids (Larson, 1988; Hou, 2002) Butylated hydroxyanisole (BHA), butylated hydroxytoluene (BHT), and propyl gallate (PG) are examples of synthetic antioxidants (Koksal and Gulcin, 2008).

Synthesis route (Scheme **1**) reported in dyes (Sheikh and Kazmi, 2017) is altered in this work. Previously, isopropylidene glycerol **(3)** was esterified with 4-(dimethylamino)benzoic acid to form **(7)** which served as coupling component for diazonium compound. Here, direct esterification of glycerol at $1^o$ OH with –COOH of 4-(dimethylamino)benzoic acid was achieved.

## MATERIALS AND METHODS

### Materials

Solvents and reagents that were used in synthesis were obtained from Sigma-Aldrich Chemical Compny, USA and Merck Millipor. Solvents were dried using standard techniques and wer of analytical grade. IR spectras were obtained using KBr discs on Jasco-320 spectrophotometer. Thermoscientific evolution-300 spectrophotometer was used for obtained UV-V spectras. $^1$H-NMR spectra were obtained in $CDCl_3$ as solvent with $Si(CH_3)_4$ added as reference at 400 and 500 MHz. NMR spectroscopy was performed on Bruker Avance AM spectrometers. QSTAR XL LC-MS mass spectrometer was used for ESI-MS. TLC or Thin layer chromatography technique was utlized to monitor the reaction progress and purity of product molecules. It was performed on 60 $F_{254}$ 20 x 20 cm Al card sheets precoated with Merck Silica gel and spots were observed under 254 and 366 nm UV light .

### Computational Methods

All calculations were performed in Gaussian09, (Frisch *et al*, 2009) and used the 6-31+G(d) basis set, along with the IEFPCM continuum solvation model for tetrahydrofuran (Tomasi *et al*., 2005) The excited state calculations used the CAM-B3LYP functional, which better models long-range interactions important for charge-transfer effects (Yanai *et al*., 2004) To plot the calculated spectrum, the frequencies and oscillator strengths of the calculated excitations were used to construct the spectrum as a sum of Gaussian functions. A peak broadening coefficient was chosen that resulted in the smallest deviation from the observed spectrum. Although a Franck-Condon analysis would have provided a more precise estimate of the peak widths, such an analysis was beyond the scope of this study.

### Synthesis

Compound **(8-10)** were synthesized using methodology devised (Scheme **1**). Metal coordinates **(11-13)** were formed as shown in (Scheme **2**).

*2,3-Dihydroxypropyl 4-(dimethylamino)benzoate* **(5)**

Carbonyldiimidazole, CDI (5 x $10^{-3}$ mol) was stirred in THF (30 ml) solvent. After complete solubility, equimolar amount of 4-(dimethylamino)benzoic acid was added to it. After stirring the mixture for 2 hours, the acyl imidazole **(4)** was added slowly to a vessel containing glycerol **(1)** (0.0125 mol) along with triethylamine base (0.52 ml) in DMSO (10 ml). Reaction mixture was stirred for further 48 hours. THF was then evaporated and obtained product was stirred in $Na_2CO_3$ solution (0.05 M). The precipitate was filtered and stirred in water, extracted with diethyl ether and was dried over added anhydrous $Na_2SO_4$. Diethyl ether was evaporated to afford the ester product **(5)**.

*2,3-dihydroxypropyl 4-(dimethylamino)-3-(phenyldiazenyl)benzoate* ***(8)***

Same method as has been devised by Sheikh and Kazmi (2017) was used for synthesis of (8-10).

### Metal Coordination:

A general method was used glycol azo metal coordination. Compound **(8-10)** (1 x $10^{-3}$ mol) was stirred in Et-OH and $H_2O$ binary solvent (1:1) along with $Na_2CO_3$ (1 x $10^{-3}$ mol) . Anhydrous $CuCl_2$ solution in Et-OH was added to the solution of **(8)** dropwise. Reaction mixture was stirred for further 24 hours after which dark colored precipitate of diol metal complex was filtered.

From the elemental analysis and mass spectra (MALDI-TOF) the glycol ligand was found to serve as a bidentate coordination lewis base. General formula is established as $M(L)_nX_2$, where L= **(8-10)**, M = Cu, n = 1 and X = Cl.

### Bioactivity

### Preparation of Solution

Extract was dissolved in 6% dimethylsulfoxide (DMSO) to afford concentration of 100 mg/ml. Gentamycin was used as reference standard (positive control). 6% dimethylsulfoxide (DMSO) served as negative control.

### DPPH Radical Scavenging Activity:

The free radical scavenging activity was obtained for 1,1-diphenyl-2-picryl-hydrazil (DPPH) by the methodology described by (Gulcin *et al*., 2005). The DPPH sol. 0.3 mM, was made in Et-OH. Each sample‘s 5 μL of different concentrations (62.5 μg - 500 μg) was stirred in 95 μl of DPPH solution in Et-OH. Mixture was dispersed in 96 well plate, later incubated at 37° C for 30 minutes. The absorbance (515) nm was obtained by microtitre plate reader (Spectramax-plus 384 Molecular Device). The % radical scavenging activity was achieved in comparison with Me-OH treated control. BHA is used as standard.

DPPH scavenging effect (%) = (Ac – As)/Ac × 100
Ac = Absorbance of Control (DMSO treated)
As = Absorbance of Sample

## RESULTS AND DISCUSSION

### Synthesis

Synthesis involved esterification of an activated arene 4-(dimethylamino)benzoic acid with $1^o$ OH of Glycerol **1**. This chemioselective esterification was achieved by slow addition of **(4)** to **(1)** which also contained $N(CH_3)_3$ base. This addition afforded **(5)**. $N(CH_3)_2$ substituent on aromatic ring of ester activates the ring towards electrophilic aromatic substitution but it is not nucleophilic or basic otherwise it would have interfered in the esterification step. For esterification, COOH of 4-(dimethylamino)benzoic acid was turned into acyl imdiazole form **(4)** by reaction with 1, 1'-carbonyldimidazole (Verma *et al*, 2012; Klemm and Heinze, 2006) Compound **(5)** was then azo coupled with diazonium ions of aniline derivatives to afford the compounds **(8-10)** (Scheme **1**). Diol Lewis basic sites of these molecules were coordinated with metal cations of Cu and Ni (Scheme **2**). Diol Lewis sites of a glycol have been coordinated with metal cations in past (Knetsch and Groenveld, 1973). 1H-NMR values of **(9)** are shown in (Fig **2.)**

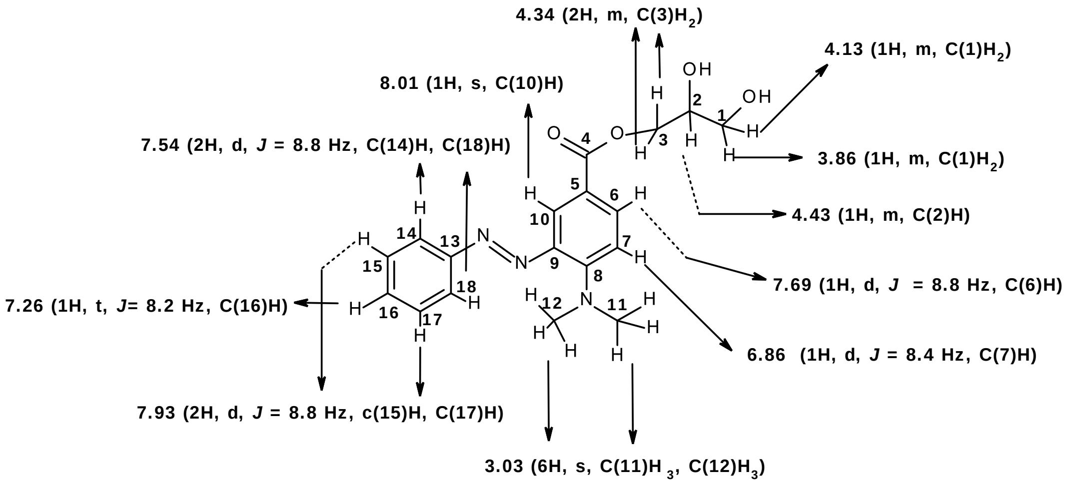

Fig. 2. $^1$H-NMR spectra of **(9)**

### Computational Results

### Dipole moment

Molecule **(9)** had a large dipole moment of 7.764 Debye, mostly due to the partial positive charge on the dimethylamino group and the partial negative charge on the ester group, with smaller contributions from the polarized glycerol C-O bonds. This large dipole moment can facilitate dipole-dipole and dipole-induced dipole interactions with the receptive sites on substrate, thus leading to strong binding.

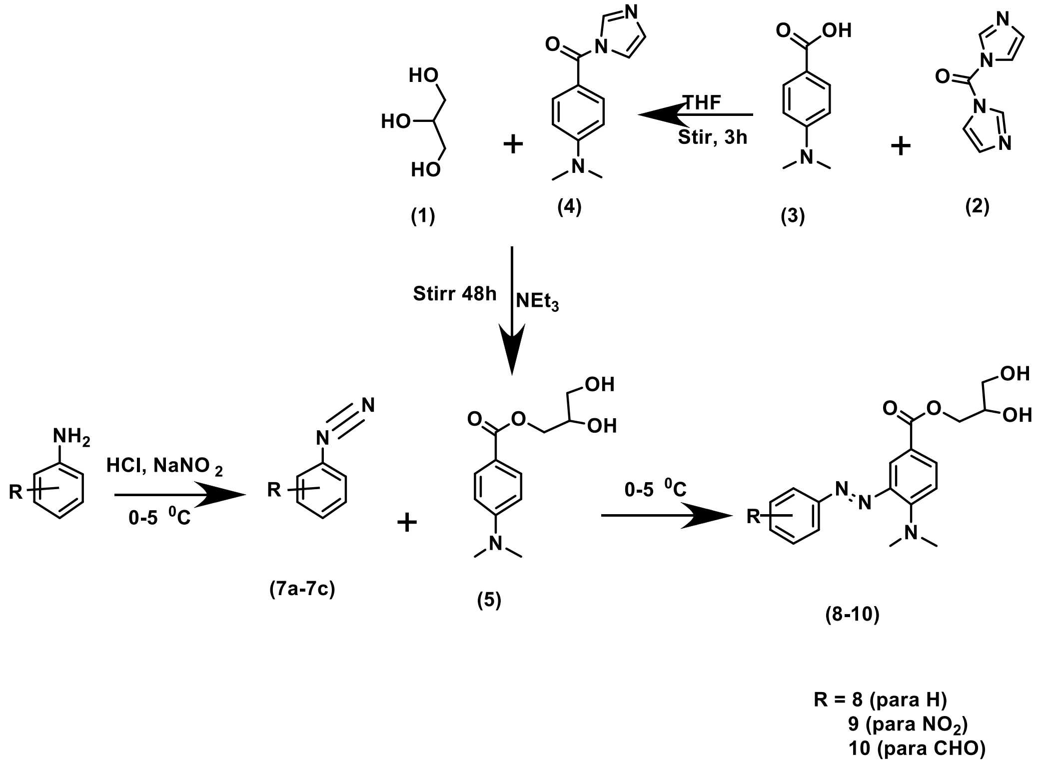

Scheme 1. Synthesis of Azo Glycol derivatives.

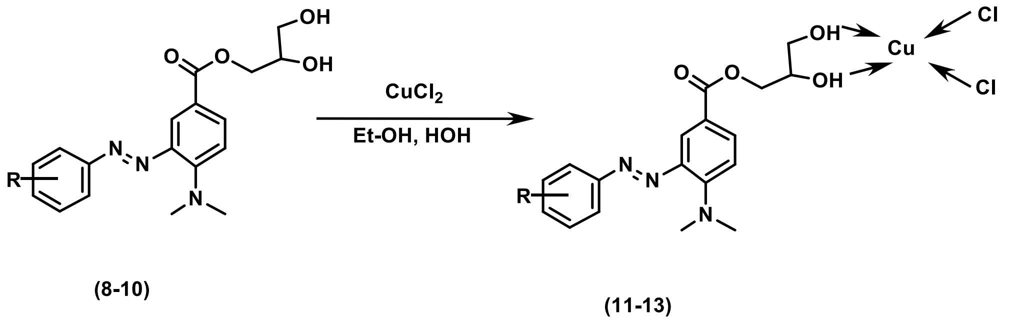

Scheme 2. Metal coordination of glycol moiety.

### TD-DFT

In order to gain insight into the basis for chromophore characteristics, TD-DFT calculations were performed with the goal of qualitatively assigning observed UV absorption bands to electronic transitions. Since the UV absorption spectrum was measured using a dilute solution of the compound in the THF, the calculations were performed in a similar context using an implicit solvation model so that a direct comparison could be made between the observed and calculated spectra (Fig 3).

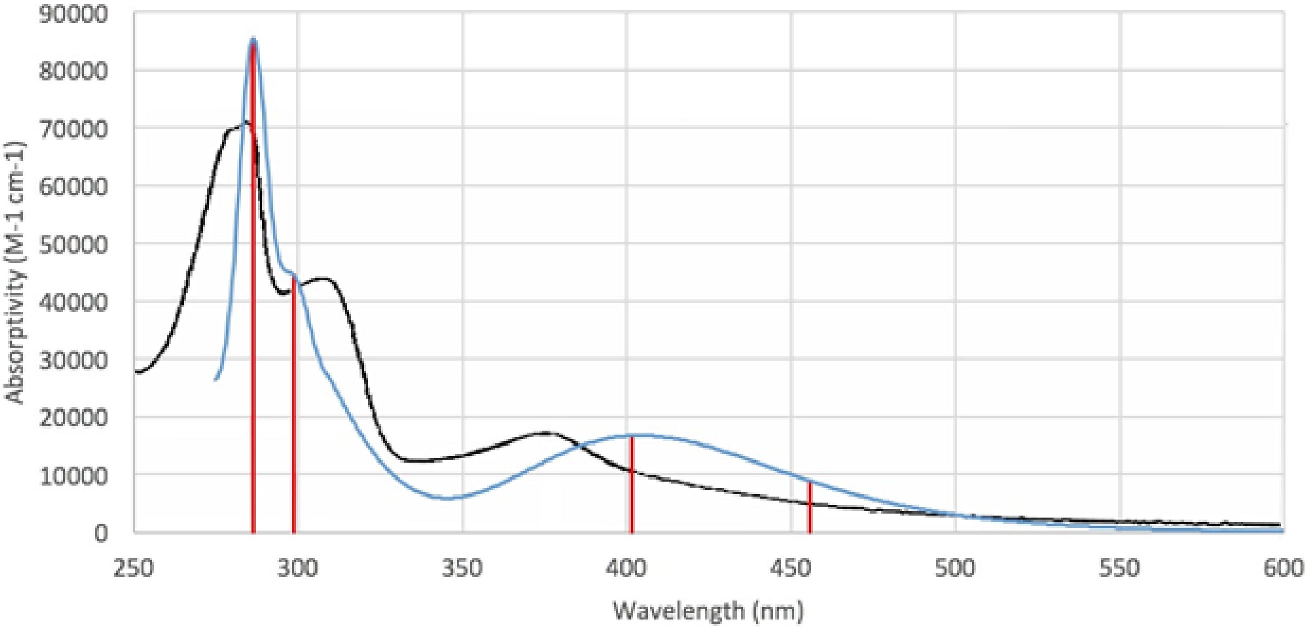

Fig 3. Calculated (blue) and observed (black) absorption spectra for compound (8) in dilute THF solution. Red vertical lines represent wavelengths of calculated electronic transitions.

The computational model was sufficiently accurate to capture the qualitative characteristics of the absorption spectrum, thus providing insights into how the spectrum depends on the molecular structure. The molecular orbitals involved in the transitions between ground and excited states were also determined (Fig **4**). The calculations showed that the main contributors were the HOMO and LUMO, but the HOMO-1, HOMO-2, LUMO+1, and LUMO+2 were also involved to varying extents in the different electronic excitations. The computed transitions matched the observed spectrum to within 0.2 eV.

The ester and diazo lone pairs, π, and π* orbitals, along with the dimethylamino lone pair and aromatic π and π* orbitals, were the main contributors to these orbitals. This indicates that these features are important in determining the absorption spectrum of the molecule.

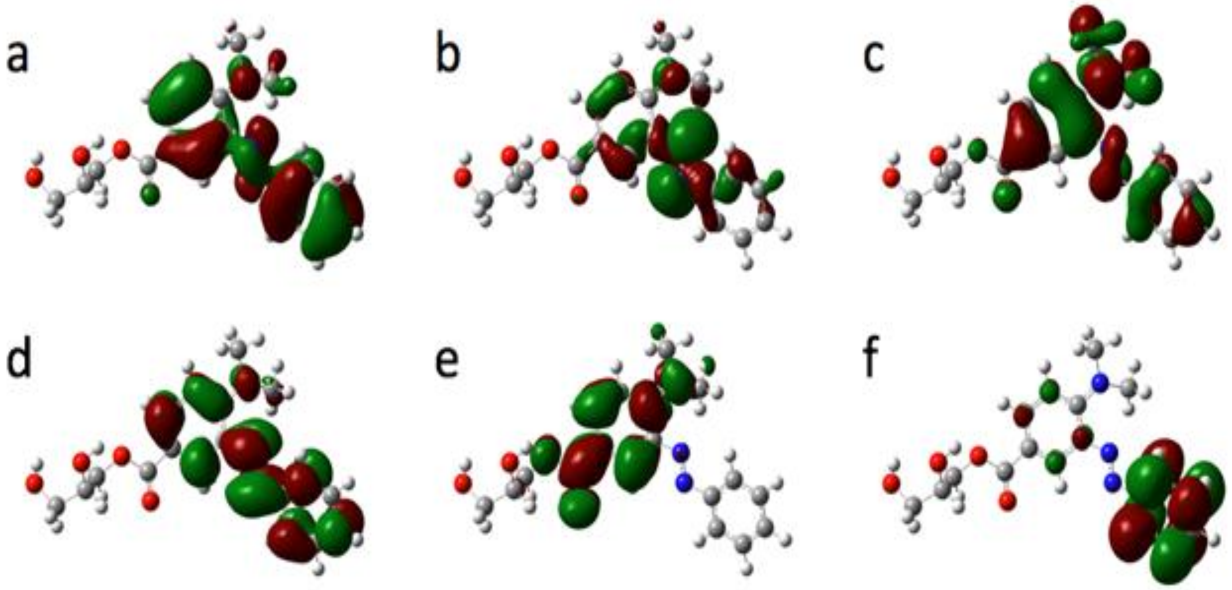

Fig 4. Molecular orbitals of compound (8). (a) HOMO-2, (b) HOMO-1, (c) HOMO, (d) LUMO, (e) LUMO+1, (f) LUMO+2.

Table 1. $^1$H-NMR Spectral Data (7-10).

| $^1$H | Integral | Coupling Constant (Hz) | Multiplicity | Shift (ppm) | | | |
|---|---|---|---|---|---|---|---|
| | | | | 7 | 8 | 9 | 10 |
| $C_1H_2$-O- | 1H | - | m | 3.86 | 3.88 | 3.86 | 3.86 |
| $C_1H_2$-O- | 1H | - | m | 4.13 | 4.14 | 4.13 | - |
| $C_3H_2$-O- | 2H | - | m | 4.34 | 4.37 | 4.34 | 4.34 |
| $C_2H$-O- | 1H | - | m | 4.43 | 4.46 | 4.43 | 4.44 |
| $C_7H, C_9H$ | 2H | $J$= 8.4 | d | 6.92 | 6.82 | 6.86 | 7.49 |
| $C_6H, C_{10}H$ | 2H | $J$ = 8.8 | d | 7.98 | 7.92,<br>8.16 | 8.01,<br>7.69 | 8.02,<br>7.89 |
| $C_{16}H$ | 1H | $J$= 8.2 | t | - | 7.26 | - | - |
| $C_{11}H_3, C_{12}H_3$ | 6H | - | s | 3.05 | 3.05 | 3.03 | 3.05 |
| $C_{15}H, C_{17}H$ | 2H | $J$ = 8.2 | t | - | 7.65 | 7.93 | 8.01 |
| $C_{14}H, C_{18}H$ | 2H | $J$= 8.2 | d | - | 8.00 | 7.54 | 7.97 |
| $C_{20}H_3$ | 3H | - | s | - | - | - | 2.59 |

Table 2. Physical and spectral data for (8-10).

| S.No | Color | Yield | M.P | (+)ESI-MS $[M+H]^+$ | Elemetal Analysis found(Calc.) | | | | $\lambda_{max}$ | $\varepsilon_{max}$ | IR (KBr) $\nu_{max}$ (cm$^{-1}$) | | | | | |
|---|---|---|---|---|---|---|---|---|---|---|---|---|---|---|---|---|
| | | % | $^0$C | m/z | C% | H% | N% | O% | nm | L mol$^{-1}$ cm$^{-1}$ | O-H | C=O | C=C | N=N | C-O ester | (C-N amine) |
| 7 | White solid | 95 | 90 | 240.1 | - | - | - | - | 310.0 | 49450.2 | 3459.0 | 1693.0 | 1611.81 | | 1277.5 | 1206.1 |
| 8 | Bright yellow | 70 | 130 | 344.1 | 62.92<br>(62.96) | 6.11<br>(6.16) | 12.29<br>(12.24) | 18.59<br>(18.64) | 380.0 | 24180.6 | 3443.4 | 1697.0 | 1606.3 | 1519.0 | 1280.1 | 1118.1 |
| 9 | Bright Red | 76 | 135 | 389.1 | 55.64<br>(55.67) | 5.18<br>(5.19) | 14.45<br>(14.43) | 24.70<br>(24.72) | 494.0 | 60194.1 | 3442.7 | 1697.2 | 1608.5 | 1514.0 | 1278.7 | 1118.1 |
| 10 | Rust | 65 | 130 | 386.1 | 62.34<br>(62.33) | 6.00<br>(6.01) | 10.88<br>(10.90) | 20.77<br>(20.76) | 415.0 | 41265.4 | 3442.7 | 1693.4,<br>1680.0<br>(ketone) | 1608.5 | 1519.8 | 1274.9 | 1188.1 |

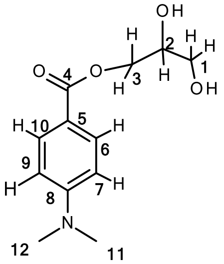

*2,3-dihydroxypropyl 4-(dimethylamino)-3-(phenyldiazenyl)benzoate **(8)***

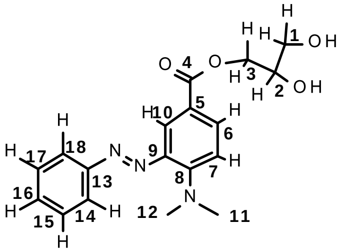

*2,3-dihydroxypropyl4-(dimethylamino)-3-((2-hydroxy-5-nitrophenyl)diazenyl)benzoate **(9)***

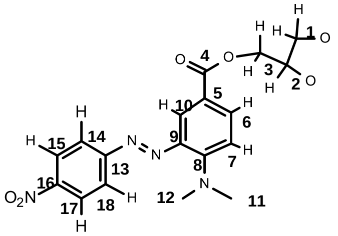

*2,3-dihydroxypropyl 3-((3-acetamidophenyl)diazenyl)-4-(dimethylamino)benzoate **(10)***

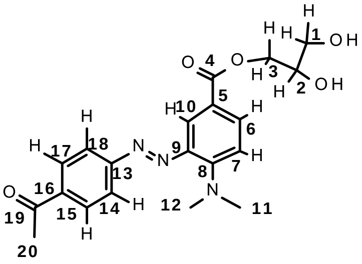

Table 3. Antioxidant activity and Urease inhibition result.

| Sr. # | Compound | Antioxidant ($IC_{50}$ ± SEM µM) [a] | Percent Inhibition at 100 uM |
|---|---|---|---|
| | 8 | 18.1 ± 0.43 | 97.5 % |
| | 9 | 22.0 ± 0.13 | 92.6% |
| | 10 | 19.4 ± 0.34 | 96.3% |
| | 11 | 35.2 ± 0.22 | 85.2 % |
| | 12 | 41.8 ± 0.11 | 77.9 % |
| 6. | 13 | 36.7± 0.35 | 82.8 % |
| | BHA std.* | 44.2 ± 0.09 | 92.3% |

a = (Mean ± Standard error of mean), Std. = Standard

Table 4. Physical and spectral data for (11-13).

| **Compound** | **Color** | **Yield** | **$[M+H]^+$** | **Elemetal Analysis found(Calc.)** | | | | | |
|---|---|---|---|---|---|---|---|---|---|
| | | **%** | **m/z** | **C%** | **H%** | **N%0** | **O%** | **Cl%** | **Cu%** |
| Cu(**8**)$_1$Cl$_2$ | Orange | 55 | 478.8 | 45.16<br>(45.24) | 4.74<br>(4.43) | 8.76<br>(8.79) | 13.36<br>(13.39) | 14.85<br>(14.84) | 13.21<br>(13.30) |
| Cu(**9**)$_1$Cl$_2$ | Maroon | 60 | 523.8 | 41.66<br>(41.35) | 3.88<br>(3.86) | 10.77<br>(10.72) | 18.39<br>(18.35) | 13.57<br>(13.56) | 12.19<br>(12.15) |
| Cu(**10**)$_1$Cl$_2$ | Brown | 82 | 520.8 | 46.31<br>(46.12) | 4.68<br>(4.64) | 8.04<br>(8.07) | 15.38<br>(15.36) | 13.66<br>(13.61) | 12.28<br>(12.20) |

## CONCLUSION

We designed bioactive novel azo glycol metal derivatives through multistep synthesis scheme. Presence of vicinal diol on the edge of the molecule can form hydrogen bonds and establish Van Der Waal interaction strong interaction with polar receptive sites on the substrate. Electronic spectral transitions were assigned using TD-DFT calculations. Dipole moment of the molecule **(8)** was also determined. High DPPH scavenging was achieved by glycol azo deriatives which slightly decreased upon their coordination with Cu.

### Acknowledgements

The authors acknowledge the contribution of Minnesota Supercomputing Institute (MSI) at the University of Minnesota for providing required resources to produce research results reported within this paper.

### Author Contribution Statement

Hamdullah Khadim Sheikh* (Synthesis, Spectroscopy, Preparation of manuscript)
Merrick Pierson-Smela (Computational modeling)
Tanzila Arshad (Synthesis, Spectroscopy)
Mehdi Hasan Kazmi (Project management)
Dr. Mehreen Lateef (Antioxidant activity)

## REFERENCES

Armstrong, D., R.S. Sohal, R.G Cutler and T.F. Slayer (1985). *Free Radicals in Molecular Biology, Aging and Discases*. Raven press, New York.

Bagchi, K. and S. Puri (1998). Free radicals and antioxidants in *health* and disease: a review. *East. Meditrr. Health. J.*, 4: 350–360.

Christen, Y., J. Am (2000). Oxidative stress and Alzheimer's disease. *Clin. Nutr*, 71: 621-629.

Frisch, M. J., G. W. Trucks, H. B. Schlegel, G. E. Scuseria, M. A. Robb, J. R. Cheeseman, G. Scalmani, V. Barone, G. A. Petersson, H. Nakatsuji, X. Li, M. Caricato, A. Marenich, J. Bloino, B. G. Janesko, R. Gomperts, B. Mennucci, H. P. Hratchian, J. V. Ortiz, A. F. Izmaylov, J. L. Sonnenberg, D. Williams-Young, F. Ding, F. Lipparini, F. Egidi, J. Goings, B. Peng, A. Petrone, T. Henderson, D. Ranasinghe, V. G. Zakrzewski, J. Gao, N. Rega, G. Zheng, W. Liang, M. Hada, M. Ehara, K. Toyota, R. Fukuda, J. Hasegawa, M. Ishida, T. Nakajima, Y. Honda, O. Kitao, H. Nakai, T. Vreven, K. Throssell, J. A. Montgomery, Jr., J. E. Peralta, F. Ogliaro, M. Bearpark, J. J. Heyd, E. Brothers, K. N. Kudin, V. N. Staroverov, T. Keith, R. Kobayashi, J. Normand, K. Raghavachari, A. Rendell, J. C. Burant, S. S. Iyengar, J. Tomasi, M. Cossi, J. M. Millam, M. Klene, C. Adamo, R. Cammi, J. W. Ochterski, R. L. Martin, K. Morokuma, O. Farkas, J. B. Foresman, and D. J. Fox, (2009). *Gaussian 09*, Gaussian, Inc., Wallingford CT.

Gulcin, I., H.A. Alici and M. Cesur (2005). Determination of in vitro antioxidant and radical scavenging activities of propofol. *Chem Phar Bull*, 53: 281-285.

Hou, W. C. (2002). Yam (Dioscorea batatas) tuber mucilage exhibited antioxidant. *Planta Med.*, 68: 1072.

Sheikh, H. K. and M. H. Kazmi (2017). Synthesis of novel 1, 2-diol containing azo dyes for polymeric substrates. *Journal of the Chilean chemical society*, 62(2): 3496-3500.

Klemm, D. and T. Heinze (2006). *Polysaccharides II*. Springer, Berlin.

Knetsch, D. and W. Groeneveld (1973). Cheminform abstract: alcohols as ligands part 3, complexes of ethylene glycol with some divalent metal halides. *Chemischer Informationsdienst*, 4(34): 81-87.

Koksal, E. and I. Gulcin, (2008). Antioxidant activity of cauliflower (Brassica oleracea L.). *Turk. J. Agric. For*. 32: 65–78.

Larson, R. (1988). The antioxidants of higher plants. *Phytochemisrty,* 27: 969-978.

Rice-Evans, C. and A.T. Diplock (1991). *Techniques in free radical research*. Elsevier, Amsterdam.

Tomasi, J., B. Mennucci and R. Cammi (2005). Quantum Mechanical Continuum Solvation Models. *Chem. Rev.*, 105: 2999–3094.

Verma, S. K., R. Ghorpade, A. Pratap and M. Kaushik (2012). Solvent free, N,N′-carbonyldiimidazole (CDI) mediated amidation. *Tetrahedron Lett.*, 53: 2373-2376.

Yanai, T., D.P. Tew and N. C. Handy (2004). A new hybrid exchange-correlation functional using the Coulomb-attenuating method (CAM-B3LYP). *Chem. Phys. Lett.*, 393: 51–57.

(*Accepted for publication May 2018*)